Functional connectivity of the anterior cingulate cortex in depression and in health

Supplementary Material

Edmund T. Rolls[2,3,#]; Wei Cheng[1,#]; Weikang Gong[1,#], Jiang Qiu[4,5,#]; Chanjuan Zhou[8,14,#]; Jie Zhang[1]; Wujun Lyu[13]; Hongtao Ruan[1,12]; Dongtao Wei[5]; Ke Cheng[8,15]; Jie Meng[5]; Peng Xie[8,9,10,*]; Jianfeng Feng[1, 2, 12,*]

Cerebral Cortex (2018) doi: 10.1093/cercor/bhy236

1. Institute of Science and Technology for Brain-inspired Intelligence, Fudan University, Shanghai, 200433, China
2. Department of Computer Science, University of Warwick, Coventry CV4 7AL, UK
3. Oxford Centre for Computational Neuroscience, Oxford, UK
4. Key Laboratory of Cognition and Personality (SWU), Ministry of Education, Chongqing, China
5. Department of Psychology, Southwest University, Chongqing, China
6. Institute of Neuroscience, Chongqing Medical University, Chongqing, China
7. Chongqing Key Laboratory of Neurobiology, Chongqing, China
8. Department of Neurology, The First Affiliated Hospital of Chongqing Medical University, Chongqing, China
9. School of Mathematical Sciences, School of Life Science and the Collaborative Innovation Center for Brain Science, Fudan University, Shanghai, 200433, PR China
10. School of Mathematics, Shanghai University Finance and Economics, Shanghai, 200433, PR China
11. Department of Neurology, Yongchuan Hospital of Chongqing Medical University, Chongqing, China
12. College of Basic Medical Sciences, Chongqing Medical University, Chongqing, China

[#] These authors contributed equally to this work.

Participants

There were 282 patients with a diagnosis of major depression, and 254 controls. The patients were from Xinan (First Affiliated Hospital of Chongqing Medical School in Chongqing, China). All participants were diagnosed according to the Diagnostic and Statistical Manual of Mental Disorder-IV criteria for major depressive disorder. Depression severity and symptomatology were evaluated by the Hamilton Depression Rating Scale (HAMD, 17 items) (Hamilton 1960) and the Beck Depression Inventory (BDI) (Beck and Beamesderfer 1974). Table S1 provides a summary of the demographic information and the psychiatric diagnosis (showing how they were diagnosed) of the participants. The data collection was approved by the local ethical review committees, was in accordance with the Code of Ethics of the World Medical Association (Declaration of Helsinki), and informed consent was obtained. This is a subset of patients from our previous functional connectivity investigation (Cheng et al. 2016), but the analysis used here is completely different and novel in its application to depression. With respect to age and sex, Table S2 shows that there were no significant differences in the age and sex of the depressed groups and the controls. Further, the effects of age and sex were regressed out in all analyses. 125 of the patients were not receiving medication at the time of the neuroimaging. Further details follow.

Patients with MDD were recruited from the outpatient department of the First Affiliated Hospital of Chongqing Medical School in Chongqing, China. All were diagnosed according to the Structured Clinical Interview for DSM-IV, by independent assessments of two psychiatrists. They were also assessed for disease severity using the Hamilton Depression Rating Scale (HAMD) (Hamilton 1960) and Beck Depression Inventory (BDI), illness duration and the medication status of the patients. Before the investigation, we excluded individuals who were not suitable for MRI scanning by interview and by the self-reported checklist. The MRI related exclusion criteria include claustrophobia, metallic implants, Meniere's Syndrome and a history of fainting within the previous half year. Exclusion criteria for both groups were as follows: current psychiatric disorders (except for MDD) and neurological disorders; substance abuse; and stroke or serious encephalopathy. Of note, all of the subjects in the control group did not meet DSM-IV criteria for any psychiatric disorders and did not use any drugs that could affect brain function. This study was approved by the Research Ethics Committee of the Brain Imaging Center of Southwest University and First Affiliated Hospital of Chongqing Medical School. Informed written consent was obtained from each subject. This study was conducted in accordance with the Helsinki Declaration as revised in 1989.

Image Acquisition

All images were acquired on a 3.0-T Siemens Trio MRI scanner using a 16-channel whole-brain coil (Siemens Medical, Erlangen, Germany). High- resolution T1-weighted 3D images were acquired using a magnetization-prepared rapid gradient echo (MPRAGE) sequence (echo time (TE) = 2.52 ms; repetition time (TR) = 1900 ms; inversion time (TI) = 900 ms; flip angle = 9 degrees; slices = 176; thickness = 1.0 mm; resolution matrix = 256×256; voxel size = 1×1×1 mm3). For each participant, 242 functional images were acquired with a gradient echo type Echo Planar Imaging (EPI) sequence (echo time (TE) = 30 ms; repetition time (TR) = 2000 ms; flip angle = 90 degrees; slices = 32; slice thickness = 3.0 mm; slice gap = 1 mm; resolution matrix = 64×64; voxel size 3.4×3.4×3mm^3). During image acquisition, participants were instructed to keep their eyes closed while keeping their head as still as possible without falling asleep. All participants stayed awake during the MRI imaging as confirmed by the participants after the session.

Data Preprocessing

Data for resting state functional connectivity analysis were collected in 3T MRI scanners in an 8 min period in which the participants were awake in the scanner not performing a task using standard protocols described in the Supplementary Material.

Data preprocessing was performed using DPARSF (Chao-Gan and Yu-Feng 2010) (http:// restfmri.net) which is a toolbox based on the SPM8 software package. The first 10 EPI scans were discarded to suppress equilibration effects. The remaining scans of each subject underwent slice timing correction by sinc interpolating volume slices, motion correction for volume to volume displacement, spatial normalization to

standard Montreal Neurological Institute (MNI) space using affine transformation and nonlinear deformation with a voxel size of $3 \times 3 \times 3mm^3$, followed by spatial smoothing (8 mm Full Width Half Maximum FWHM). To remove the sources of spurious correlations present in resting-state BOLD data, all fMRI time-series underwent band-pass temporal filtering (0.01-0.1 Hz), nuisance signal removal from the ventricles, and deep white matter, and regressing out any effects of head motion using the Friston et al 24 head motion parameters procedure (Friston et al. 1996). Finally, we implemented additional careful volume censoring ("scrubbing") movement correction as reported by Power et al. (Power et al. 2014) to ensure that head-motion artifacts are not driving observed effects. The mean framewise displacement (FD) was computed with FD threshold for displacement being 0.5. In addition to the frame corresponding to the displaced time point, 1 preceding and 2 succeeding time points were also deleted to reduce the spill-over effect of head movements. Subjects with >10% displaced frames flagged were completely excluded from the analysis as it is likely that such high-level of movement would have had an influence on several volumes. Global signals were not regressed out, for reasons described elsewhere (Cheng *et al.* 2016). Considering the potential effect of gender (Tomasi and Volkow 2012), age (Geerligs et al. 2015) and head motion (Power et al. 2012; Power *et al.* 2014) on functional connectivity, any effects of gender ratio, years of education, age and head motion between the patient and control groups were regressed out in all analyses. There were no differences in the gender ratios, age and mean FD ($p>0.05$ in all cases), though the number of years of education was lower in the patients than controls. However, none of the functional connectivity link differences found between patients and controls was correlated significantly (FDR $p<0.05$) with the number of years of education.

Table S1. A summary of the demographic information and the psychiatric diagnosis in the present study.

Group	Age (years)	Sex (male/female)	Education (years)	Medication (yes / no)	HAMD	BDI	Duration of illness	First episode (yes / no)	Mean FD
Healthy	39.65 ± 15.80	166 / 88	13.01 ± 3.89	/	/	/	/	/	0.133 ±0.063
Patient	38.74 ± 13.65	183 / 99	11.91 ± 3.58	157 / 125	20.8 ± 5.87	20.42 ± 9.33	4.16 ± 5.51	209 / 49	0.125 ± 0.054
Statistic (t / p) or (chi-square / p)	0.719 / 0.472	0.013 / 0.911	3.41 / 6.9e-4	/	/	/	/	/	1.729 / 0.084
Unmedicated patient	37.60 ± 13.12	84 / 41	12.07 ± 3.72	125 / 0	22.22 ± 4.39	22.51 ± 8.16	2.91 ± 4.44	111 / 14	0.120 ± 0.053
Medicated patient	39.64 ± 14.03	99 / 58	11.78 ± 3.48	0 / 157	19.42 ± 6.73	18.43 ± 9.95	5.33 ± 6.13	98 / 35	0.129 ± 0.054
Statistic (t / p) or (chi-square / p)	-1.250 / 0.212	0.524 / 0.469	0.673 / 0.501	/	3.907 / 1.2e-4	3.520 / 5.1e-4	-3.539 / 4.8e-4	9.570 / 0.002	-1.268 / 0.206

Values are n or mean ± SD.

Note: The difference between patients and controls for continuous variables was assessed by a two-sample t-test and the difference for the binary variable (gender) was assessed by a chi-square test.

Age, education, HAMD, BDI, duration of illness and Mean FD are presented in mean ± SD.

HAMD = Hamilton Depression Rating Scale;

BDI = Beck Depression Inventory

Mean FD = mean framewise displacements.

Table S2. The anatomical regions defined in each hemisphere and their label in the automated anatomical labelling atlas AAL2 (Rolls et al. 2015). Column 4 provides a set of possible abbreviations for the anatomical descriptions.

NO.	ANATOMICAL DESCRIPTION	LABEL aal2.nii.gz	POSSIBLE ABBREVIATION
1,2	Precentral gyrus	Precentral	PreCG
3, 4	Superior frontal gyrus, dorsolateral	Frontal_Sup	SFG
5, 6	Middle frontal gyrus	Frontal_Mid	MFG
7, 8	Inferior frontal gyrus, opercular part	Frontal_Inf_Oper	IFGoperc
9, 10	Inferior frontal gyrus, triangular part	Frontal_Inf_Tri	IFGtriang
11, 12	IFG pars orbitalis,	Frontal_Inf_Orb	IFGorb
13, 14	Rolandic operculum	Rolandic_Oper	ROL
15, 16	Supplementary motor area	Supp_Motor_Area	SMA
17, 18	Olfactory cortex	Olfactory	OLF
19, 20	Superior frontal gyrus, medial	Frontal_Sup_Med	SFGmedial
21, 22	Superior frontal gyrus, medial orbital	Frontal_Med_Orb	PFCventmed
23, 24	Gyrus rectus	Rectus	REC
25, 26	Medial orbital gyrus	OFCmed	OFCmed
27, 28	Anterior orbital gyrus	OFCant	OFCant
29, 30	Posterior orbital gyrus	OFCpost	OFCpost
31, 32	Lateral orbital gyrus	OFClat	OFClat
33, 34	Insula	Insula	INS
35, 36	Anterior cingulate & paracingulate gyri	Cingulate_Ant	ACC
37, 38	Middle cingulate & paracingulate gyri	Cingulate_Mid	MCC
39, 40	Posterior cingulate gyrus	Cingulate_Post	PCC
41, 42	Hippocampus	Hippocampus	HIP
43, 44	Parahippocampal gyrus	ParaHippocampal	PHG
45, 46	Amygdala	Amygdala	AMYG
47, 48	Calcarine fissure and surrounding cortex	Calcarine	CAL
49, 50	Cuneus	Cuneus	CUN
51, 52	Lingual gyrus	Lingual	LING
53, 54	Superior occipital gyrus	Occipital_Sup	SOG
55, 56	Middle occipital gyrus	Occipital_Mid	MOG
57, 58	Inferior occipital gyrus	Occipital_Inf	IOG
59, 60	Fusiform gyrus	Fusiform	FFG
61, 62	Postcentral gyrus	Postcentral	PoCG
63, 64	Superior parietal gyrus	Parietal_Sup	SPG
65, 66	Inferior parietal gyrus, excluding supramarginal and angular gyri	Parietal_Inf	IPG
67, 68	SupraMarginal gyrus	SupraMarginal	SMG
69, 70	Angular gyrus	Angular	ANG
71, 72	Precuneus	Precuneus	PCUN
73, 74	Paracentral lobule	Paracentral_Lobule	PCL
75, 76	Caudate nucleus	Caudate	CAU
77, 78	Lenticular nucleus, Putamen	Putamen	PUT
79, 80	Lenticular nucleus, Pallidum	Pallidum	PAL
81, 82	Thalamus	Thalamus	THA
83, 84	Heschl's gyrus	Heschl	HES
85, 86	Superior temporal gyrus	Temporal_Sup	STG
87, 88	Temporal pole: superior temporal gyrus	Temporal_Pole_Sup	TPOsup
89, 90	Middle temporal gyrus	Temporal_Mid	MTG
91, 92	Temporal pole: middle temporal gyrus	Temporal_Pole_Mid	TPOmid
93, 94	Inferior temporal gyrus	Temporal_Inf	ITG

Table S3. Numbers of voxels in different AAL2 areas with significantly different functional connectivity with the anterior cingulate cortex (ACC) in unmedicated patients with depression (as shown in Fig. S1). For ACC, the table shows the number of ACC voxels that have different functional connectivity with the whole brain. The other entries in the table show the numbers of voxels in each of the specified brain regions with different functional connectivity with ACC voxels.

Areas	# Voxels	Peak value*	MNI coordinates (Peak)		
Fusiform_L, Fusiform_R, Temporal_Pole_Sup_L, Temporal_Mid_R, Temporal_Pole_Mid_L, Temporal_Inf_L, Temporal_Inf_R	156	-24	-63	-24	-27
Olfactory_R, Rectus_L, Rectus_R, OFCmed_L, OFCmed_R, OFCant_L, OFCant_R, OFCpost_L, OFCpost_R	215	47	6	21	-27
Frontal_Inf_Orb_2_L, Frontal_Inf_Orb_2_R	29	21	-27	27	-12
Frontal_Mid_2_R, Frontal_Inf_Oper_R, Frontal_Inf_Tri_R	259	378	36	18	24
Frontal_Sup_2_L, Frontal_Sup_2_R, Frontal_Med_Orb_L	112	88	24	9	45
Occipital_Sup_L, Occipital_Sup_R, Occipital_Mid_L, Occipital_Mid_R, Occipital_Inf_L	277	17	39	-78	9
Parietal_Sup_L, Parietal_Sup_R, Parietal_Inf_R	101	9	30	-51	51
Caudate_R, Putamen_R	65	-58	18	24	-3
Precentral_R, Supp_Motor_Area_R, Postcentral_L, Postcentral_R, Paracentral_Lobule_L	110	41	48	6	42
Cingulate_Ant_L, Cingulate_Ant_R	468	271	15	36	24
Precuneus_L, Precuneus_R	12	5	15	-60	48
Angular_R	16	-20	42	-66	51
Cuneus_L	8	5	-9	-90	36
Insula_L, Insula_R	18	31	45	21	0

*: the number of significantly different functional connectivity links relating to the voxels ($p<0.05$, corrected). The negative value means the FCs are decreased in patients with depression, and vice versa.

Figure S1. Anatomical location of voxels with significantly different functional connectivity with the anterior cingulate cortex when comparing the non-medicated and medicated depression (medicated patients - unmedicated patients) obtained from the voxel-based Association Study (vAS). The color bar represents the number of significantly different functional connectivity links relating to each voxel after cluster wise correction ($p<0.05$). For almost all of these voxels, the difference in functional connectivity related to the effects of medication was a decrease, and thus the measure shown here uses a blue scale.

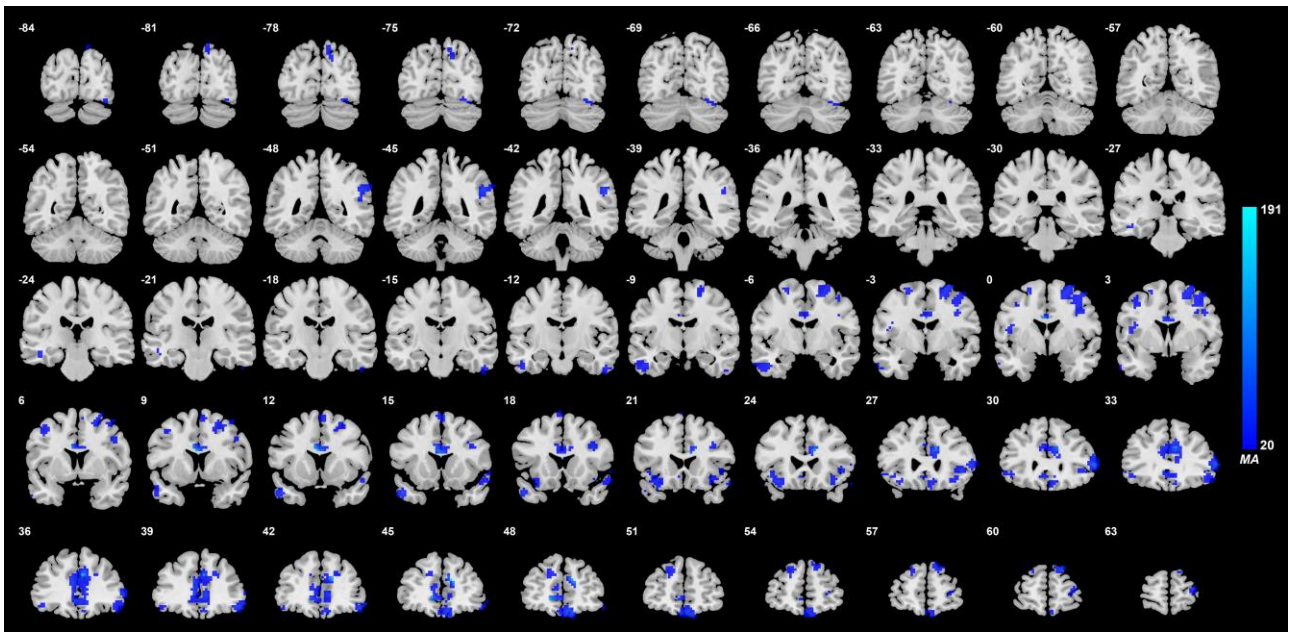

Figure S2. The voxel-level functional connectivity for anterior cingulate voxels that are significantly different in the unmedicated depressed and the control group, separated by the AAL2 region (Rolls *et al.* 2015) in which the significant voxels were located. Conventions as in Fig. 2. Red/yellow indicates voxels with predominantly increased functional connectivity in the unmedicated depressed group. A. Voxels in medial orbitofrontal cortex areas. B. Voxels in lateral orbitofrontal cortex area IFGorb and its extension towards the anterior insula. C. Voxels in the superior part of the inferior frontal gyrus (pars triangularis and pars opercularis).

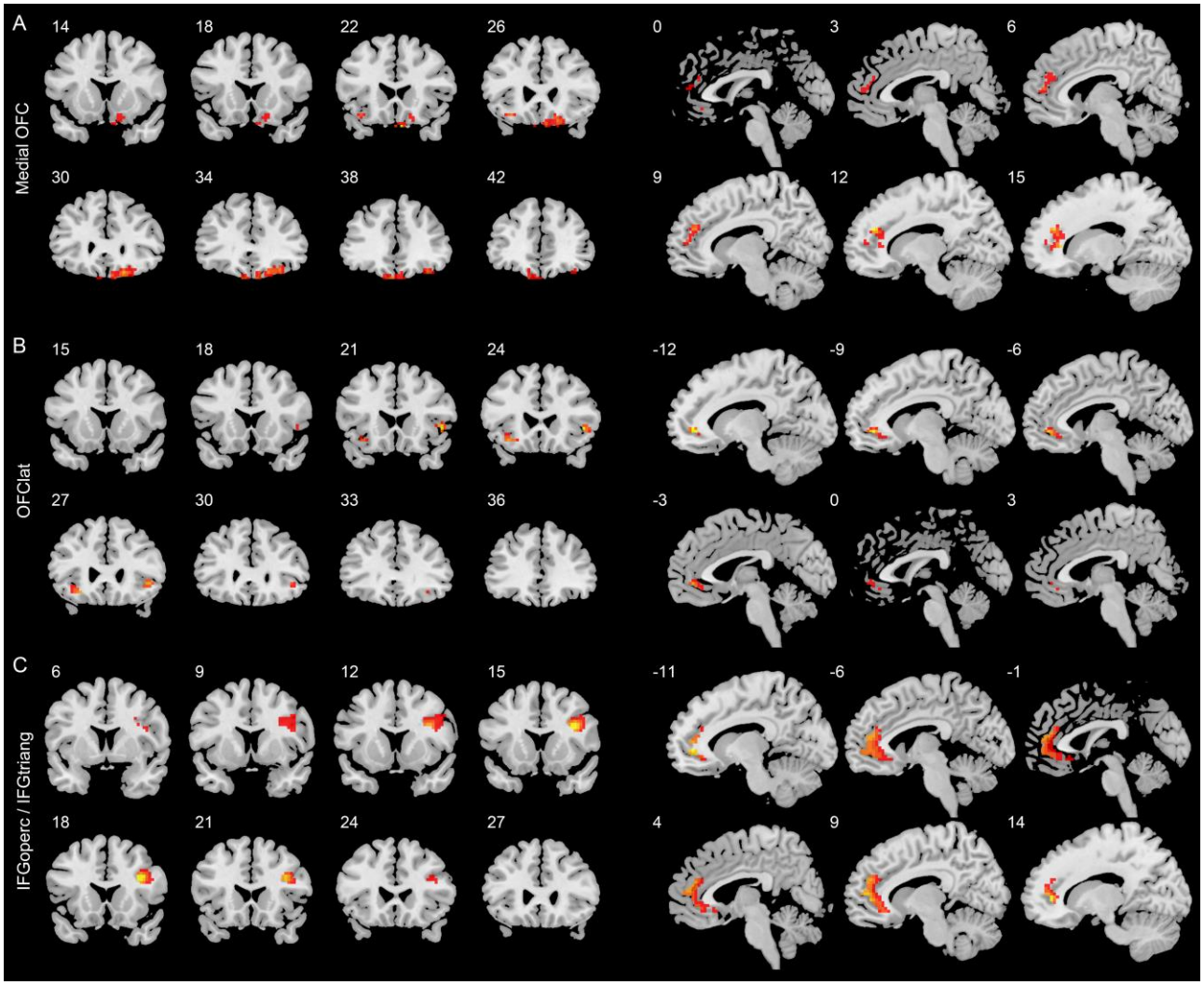

References

Beck AT, Beamesderfer A. 1974. Assessment of depression: the depression inventory. Mod Probl Pharmacopsychiatry 7:151-169.
Chao-Gan Y, Yu-Feng Z. 2010. DPARSF: a MATLAB toolbox for “pipeline” data analysis of resting-state fMRI. Front Syst Neurosci 4:13.
Cheng W, Rolls ET, Qiu J, Liu W, Tang Y, Huang CC, Wang X, Zhang J, Lin W, Zheng L, Pu J, Tsai SJ, Yang AC, Lin CP, Wang F, Xie P, Feng J. 2016. Medial reward and lateral non-reward orbitofrontal cortex circuits change in opposite directions in depression. Brain 139:3296-3309.
Friston KJ, Williams S, Howard R, Frackowiak RS, Turner R. 1996. Movement-related effects in fMRI time-series. Magn Reson Med 35:346-355.
Geerligs L, Renken RJ, Saliasi E, Maurits NM, Lorist MM. 2015. A Brain-Wide Study of Age-Related Changes in Functional Connectivity. Cereb Cortex 25:1987-1999.
Hamilton M. 1960. A rating scale for depression. J Neurol Neurosurg Psychiatry 23:56-62.
Power JD, Barnes KA, Snyder AZ, Schlaggar BL, Petersen SE. 2012. Spurious but systematic correlations in functional connectivity MRI networks arise from subject motion. Neuroimage 59:2142-2154.
Power JD, Mitra A, Laumann TO, Snyder AZ, Schlaggar BL, Petersen SE. 2014. Methods to detect, characterize, and remove motion artifact in resting state fMRI. Neuroimage 84:320-341.
Rolls ET, Joliot M, Tzourio-Mazoyer N. 2015. Implementation of a new parcellation of the orbitofrontal cortex in the automated anatomical labeling atlas. Neuroimage 122:1-5.
Tomasi D, Volkow ND. 2012. Laterality patterns of brain functional connectivity: gender effects. Cereb Cortex 22:1455-1462.